Article

Bactericidal Hydrogels via Surface Functionalization with Cecropin A

Megan A Cole, Timothy F Scott, and Charlene M. Mello

ACS Biomater. Sci. Eng., **Just Accepted Manuscript** • DOI: 10.1021/acsbiomaterials.6b00266 • Publication Date (Web): 06 Sep 2016

Bactericidal Hydrogels via Surface Functionalization with Cecropin A

Megan A. Cole[†], Timothy F. Scott[*,‡,§], and Charlene M. Mello[*,†]

[†] U.S. Army Natick Soldier Research, Development, and Engineering Center, Natick, MA 01760

[‡] Department of Chemical Engineering, University of Michigan, Ann Arbor, MI 48109

[§] Macromolecular Science and Engineering Program, University of Michigan, Ann Arbor, MI 48109

KEYWORDS. Antimicrobial peptide, cecropin A, hydrogel, immobilization, *E. coli*

ABSTRACT. The immobilization of antimicrobial peptides (AMPs) to surfaces, enabling their utilization in biosensor and antibacterial/antifouling coating applications, is typically performed using rigid, solid support materials such as glass or gold and may require lengthy, temperamental protocols. Here, we employ a hydrogel immobilization platform to afford facile fabrication and surface functionalization while offering improved biocompatibility for evaluating the influence of linker length, surface density, and AMP conjugation site on retained peptide activity. Rapid, interfacial photopolymerization using the radical-mediated thiol–ene addition mechanism was used to generate cross-linked, polymeric coatings bearing residual thiol moieties on pre-fabricated poly(ethylene glycol) (PEG)-based hydrogel supports. The photopolymerized

coatings were 60 μm thick and contained 0.55 nmol unreacted free thiols, corresponding to a concentration of 410 μM, for use as cecropin A (CPA) immobilization handles via thiol-maleimide conjugation, where the CPA-bound maleimide moiety was localized at either the carboxyl terminus or mid-sequence between Ala_{22} and Gly_{23}. Surface presentation of the thiol handles was controlled by varying the thiolated PEG monomer (PEGSH) used in the photopolymerizable formulation. Bactericidal activity of CPA functionalized hydrogels against *E. coli* K235 indicated that CPA immobilized at the carboxyl terminus killed 94±6% of the inoculated pathogens when coatings were prepared with high molecular weight PEGSH and 99±1% when prepared with low molecular weight PEGSH. *E. coli* cell death demonstrated a stronger dependence on peptide concentration than PEG linker length or degree of thiol functionalization, with activity ranging from 34±13% to 99±1% bacterial cells killed as the pre-functionalization thiol concentration in the coatings was increased from 90 μM to 990 μM. Finally, the immobilization site on the surface-bound CPA strongly affected antibacterial activity; when mid-sequence modified CPA was bound to a hydrogel coating bearing 990 μM thiol, only 20±4% of the *E. coli* population was killed.

INTRODUCTION

Antimicrobial peptides (AMPs) compose a large reservoir of naturally occurring amino acid sequences that serve as fundamental components of the immune systems of microorganisms,[1] plants,[2] insects,[3] and, to a lesser degree, mammals.[4] Most AMPs have relatively short sequences consisting of 5-40 amino acids, and contributions from lysine and arginine typically yield cationic peptides with net charges ranging from +2 to +9 at neutral pH.[5] Substantial quantities of hydrophobic residues (i.e., 30% or more total residues) and an amphipathic nature are also

common features among AMPs. Although a small fraction of AMPs target intracellular domains,[6] the hallmark mechanism of action is membrane disruption, enabling broad spectrum anti-pathogenic activity. Electrostatic interactions often initiate AMP-membrane associations, where positively-charged peptides associate with negatively-charged species in lipid bilayers and proceed to disrupt the membrane by a variety of mechanisms. For example, cationic AMPs have been shown to bind to lipopolysaccharides within Gram-negative bacterial membranes, displacing the native stabilizing divalent cations (i.e., Ca^{2+} and Mg^{2+}) and forcing the membrane to leak.[7]

Multiple mechanistic models detailing the intricacies of AMP association with and disruption of cell membranes have been proposed, but the precise pathway utilized by a particular AMP appears to be a function of numerous physicochemical properties, including the net charge, amphipathicity, and secondary structure of the peptide as well as the concentration of peptide and cell membrane composition.[8] Likewise, the strength and specificity of AMP activity coincides with the biochemical and structural characteristics of the peptide sequence. For example, whereas anionic, phosphorylated peptides such as enkelytin and peptide B are primarily active against Gram-positive bacteria,[9] proline- and glycine-rich cationic peptides typically exhibit Gram-negative selectivity.[10] Lysine-rich dermaseptins display high levels of activity towards filamentous fungi,[11] and the cysteine-rich defensins have proven effective against herpes simplex virus type 1.[12] An array of cationic AMPs has even shown specificity towards malignant tumor cells,[13] believed attributable to electrostatic interactions between positively-charged AMPs and negatively-charged cell membrane components as tumor cells frequently over express anionic membrane molecules such as phosphatidylserine and O-glycosylated mucins.[14]

Given their broad range of activities, immobilized AMPs have become increasingly attractive for detecting,[15] capturing,[16] and deactivating target pathogens.[17] However, as native AMPs occur free in solution, binding AMPs to a surface presents a unique set of obstacles to ensure their antimicrobial properties are retained. AMPs in solution may preferentially associate with cell membranes using residues on either the amino (N-) or the carboxyl (C-) terminus, or undergo a conformational change to confer activity;[18] therefore, the AMP binding orientation and substrate rigidity must be considered. Conventional approaches to covalently attach AMPs to surfaces afford varying degrees of peptide orientation control. The coupling of lysine-bearing AMPs to succinimidyl ester-functionalized glass, previously employed to assess the sensitivity of an AMP-based approach to detect heat-killed bacteria,[19] offers little orientational control since all AMPs used in that study contained multiple lysine residues distributed throughout their sequences, each of which were potential attachment sites. Alternatively, incorporation of an exogenous cysteine residue has proven particularly advantageous in controlling the site-specific attachment and orientation of immobilized peptides, as this approach enables facile Michael addition reactions that proceed between the AMP-bound cysteine residues and surface-bound maleimide linker molecules,[20] or even the fabrication of AMP monolayers by self-assembly on gold surfaces.[21] Notably, the terminus at which the cysteine residue is incorporated influences peptide orientation upon immobilization.[22] Cecropin P1 immobilized by its N-terminus has been shown to orient horizontally to its substrate at low concentrations, vertically at intermediate concentrations, and in a blend of horizontal and vertical orientations at high concentrations;[22b] however, the same peptide immobilized via a C-terminus cysteine residue adopts multiple orientations regardless of concentration.[22a]

Inclusion of a molecular linker between the solid support and the AMP provides advantages both in terms of synthetic accessibility and anti-microbial performance. Specifically, the use of a linker expands the variety of chemical reactions that may be utilized to immobilize an AMP, and overcomes the steric hindrance inherent to direct covalent attachment. Poly(ethylene glycol) (PEG) chains are commonly employed as spacers between immobilized AMPs and a diverse range of solid substrates.[17, 23] A 98% reduction in *Pseudomonas aeruginosa* populations was observed following the covalent attachment of azido-PEGylated AMPs to alkynyl groups on fluoropolymer surfaces,[24] while a 3 log reduction (i.e., 99.9%) in *E. coli* growth was found for PEG-modified poly(ethylene) films functionalized with an AMP via a carbodiimide coupling.[25] Indeed, the absence or presence of a PEG spacer was found to significantly alter the antibacterial activity of surface-immobilized chrysophsin 1, where functionalized surfaces incorporating the flexible spacer killed 82% of *E. coli* cells while only 34% of the cells were killed by AMP-surfaces that lacked the spacer group.[26]

Despite the demonstrated improvement in immobilized-AMP activity when spacer groups are employed, the relationship between spacer length and degree of peptide activity remains under-examined. Furthermore, comparison of experimental results for a singular AMP within the existing research is complicated by the lack of uniformity in peptide surface densities, strains and concentrations of pathogen(s) evaluated, and test methods used to quantify antimicrobial activity. Thus, the objective of this work is to utilize a rapid immobilization technique for the systematic characterization of the bactericidal activity of cecropin A (CPA) in a variety of surface presentations. Specifically, following conjugation of maleimide-modified CPA to thiol functional groups localized to PEG hydrogel surfaces, where the molecular weight, number of thiol groups, and surface concentration of the thiol-terminated PEG spacer were varied, the

activity of CPA against *E. coli* was evaluated. Additionally, immobilized peptide activity was examined in response to the location of the maleimide conjugation site within CPA, whereby a maleimide-modified lysine residue was inserted at either the C-terminus of the CPA sequence or within the middle of the sequence at a position that serves as a "hinge" region in the folded peptide. In both cases, analogous sequences featuring glycine residues between the native CPA sequence and the modified lysine residue were prepared to determine whether the resultant separation between the peptide and hydrogel-bound thiol conjugation site affects anti-bacterial activity by enabling folding into the active state to be more readily achieved.

MATERIALS AND METHODS

Materials. 2,4,6-Trimethylbenzoyl chloride and allyl bromide were purchased from Fisher Scientific (Franklin, MA). Dimethoxyphenylphosphine, lithium bromide, sodium hydride, poly(ethylene glycol) (PEG, M_n 10,000 g mol^{-1}), poly(ethylene glycol) diacrylate (PEGDA, M_n 700 g mol^{-1}), ethylenediaminetetraacetic acid (EDTA), Luria Bertani (LB) broth (Lennox), LB agar, sodium chloride, potassium phosphate monobasic, potassium phosphate dibasic, ammonium sulfate, trisodium citrate dihydrate, D-(+)-glucose, acetic acid, and bovine serum albumin (BSA) were purchased from Sigma Aldrich (St. Louis, MO). Three 4-arm PEG-thiols (M_n 5,000 g mol^{-1}, 10,000 g mol^{-1}, and 20,000 g mol^{-1}) and one 8-arm PEG-thiol (M_n 20,000 g mol^{-1}) were purchased from JenKem Technology (Tianjin, China). Four custom CPA sequences containing a maleimide-modified lysine residue (denoted by K^*) in one of two positions, C-terminus or mid-chain and with or without a glycine spacer (see Table 1), were purchased from New England Peptide (Boston, MA). Alexa Fluor 488 C5-maleimide, 5,5'-dithiobis-(2-nitrobenzoic acid) (Ellman's reagent), and LIVE/DEAD *Bac*Light bacterial viability kit were purchased from Life Technologies (Grand Island, NY). All materials were used as received.

Table 1. Maleimide-modified cecropin A sequences and their respective minimum inhibitory concentrations (MICs) against *E. coli* K235.

Abbreviation	Sequence	MIC (μg mL^{-1})
CPA–K*	H–KWKLFKKIEK VGQNIRDGII KAGPAVAVVG QATQIAK**K***–$CONH_2$	1.56 ± 0.00
CPA–GGGGK*	H–KWKLFKKIEK VGQNIRDGII KAGPAVAVVG QATQIAKGGG G**K***–$CONH_2$	2.61 ± 0.91
–AK*G–	H–KWKLFKKIEK VGQNIRDGII KA**K***GPAVAVV GQATQIAK–$CONH_2$	25 ± 0
–GGAK*GGG–	H–KWKLFKKIEK VGQNIRDGII KGGA**K***GGGPA VAVVGQATQI AK–$CONH_2$	>50

Lithium phenyl-2,4,6-trimethylbenzoylphosphinate (lithium acylphosphinate, LAP) was synthesized according to a previously-described method[27] in 80% yield over two steps. PEG-diallyl ether (PEGDAE) was synthesized using a modified method from the literature.[28] Briefly, dihydroxylated PEG (M_n 10,000 g mol^{-1}) was dissolved in toluene under nitrogen and excess sodium hydride was added slowly. After gas evolution, a large excess of allyl bromide was added drop-wise, and the reaction was heated to 70°C and stirred for 24 hours. The reaction mixture was then filtered and added drop-wise to cold diethyl ether. The resultant precipitate was isolated, dried, dissolved in deionized water, and dialyzed against a large volume of deionized water. Finally, the retentate was lyophilized to afford PEGDAE 10k as a white, free-flowing powder, and quantitative end-group functionalization was verified by ^{1}H NMR.

Fabrication of Hydrogel Cores and Coatings. Cross-linked PEGDA hydrogel cores were used as the underlying substrates for all antimicrobial studies. The hydrogel cores were formed from a pre-polymer solution containing PEGDA (700 g mol^{-1}, 20 wt%) and 0.05 wt% LAP as a

photoinitiator in sterilized, deionized water. 52 μL of pre-polymer was injected into a sterile 96-well microtiter plate (Greiner Bio-One, black with coverslip bottoms) and irradiated for 25 s under ultraviolet light (30 mW cm^{-2} from an Omnicure S1000 (Lumen Dynamics) equipped with a 320-390 nm filter) through a photomask featuring 3.0 mm diameter circles (2:1 aspect ratio) and adhered to the base of the microtiter plate. After polymerization, a micropipette was used to remove the unreacted pre-polymer solution, and the remaining solid hydrogel discs were rinsed with deionized water and swollen overnight in 55 μL of a 10 mM LAP solution.

After swelling, a polymer coating was formed on the hydrogel cores using a photo-mediated interfacial polymerization technique (see Scheme 1). For this process, the LAP solution surrounding the solid hydrogel was removed and, immediately after adding 55 μL of a pre-polymer immersate solution containing PEGSH and PEGDAE in a 2:1 SH:C=C ratio, the well was irradiated with ultraviolet light (5 mW cm^{-2}, 320-390 nm), initiating polymerization exclusively at the interface of the hydrogel and the pre-polymer immersate solution to generate the polymer coating.

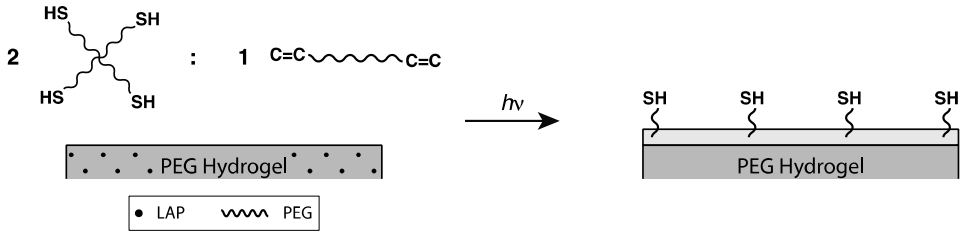

Scheme 1. Illustration of the interfacial photo-polymerization technique. The photoinitiator (LAP) and reactive monomers (PEGDAE and PEGSH) are initially spatially confined in a PEG-based hydrogel and immersate solution, respectively. Upon contact, the molecular species diffuse in opposing directions; under irradiation, LAP undergoes homolytic scission to generate

radicals that initiate thiol–ene polymerization, and affords a hydrogel coating incorporating residual, unreacted thiol groups that may be conjugated with maleimide-functionalized CPA.

The duration of light exposure was tailored for each PEGDAE and PEGSH immersate solution such that the final coating thickness was approximately 60 μm (see Table 2). Following irradiation, unreacted pre-polymer solution was removed, and the coated hydrogels were rinsed three times with sterilized, deionized water.

Coating Characterization. The thickness of the cross-linked coatings as a function of exposure time was measured by laser scanning confocal microscopy (Zeiss LSM 710). Coated hydrogels were incubated for 1 hr with Alexa Fluor 488 C5 maleimide (0.1 mM) in 0.1 M PBS (pH 7.2) to label free thiol functional groups in the coatings. The fluorescent staining solution was then replaced with deionized water to allow unreacted dye to leach out of the coated hydrogel; the leachate was replaced with fresh water every 15 min for 1 hr. The fluorescent coating was visualized by exciting at 488 nm and recording emission from 460 – 520 nm.

The amount of free thiols within the hydrogel coatings was quantified using Ellman's reagent. After removing the deionized water from wells containing coated hydrogels, 50 μL of reaction buffer (0.1 M PBS, pH 8.0, with 1 mM EDTA) and 1 μL of Ellman's reagent solution (0.4 wt/vol% Ellman's reagent in reaction buffer) were added. A reference solution was formulated from 50 μL of reaction buffer mixed with 1 μL of Ellman's reagent solution and 6 μL of deionized water. The 96-well microtiter plate was agitated for 15 min at room temperature, after which 50 μL of the test and reference solutions were transferred to separate wells in a fresh microtiter plate for absorption measurements at 412 nm using a microplate reader (SpectraMax M5, Molecular Devices). The quantities of thiol functional groups in the coatings were

calculated by the Beer-Lambert law using the molar extinction coefficient of 2-nitro-5-thiobenzoic acid (i.e., the colored cleavage species of Ellman's reagent, $\varepsilon = 14{,}150\ M^{-1}\ cm^{-1}$).[29] All measurements were performed in triplicate.

Peptide Immobilization. Cecropin A was immobilized to the hydrogel disc surfaces by reacting the maleimide functional groups on the CPA sequences with free thiols in the polymer coatings via Michael addition (Scheme 2). Surface functionalization was conducted by adding 100 μL of an aqueous solution formulated with a 10-fold molar excess of maleimide-functionalized peptide (1 mM CPA) in 0.1 M PBS (pH 7.2) to each hydrogel well. The microtiter plates housing the hydrogels and CPA solutions were agitated for 15 min and incubated overnight at 4°C. After removing the buffer solution, the hydrogels were rinsed three times with sterile deionized water and placed under agitation for 1 hr with deionized water replacement every 15 min. Negative control samples were treated identically using sterile 0.1 M PBS (pH 7.2) that excluded the maleimide-functionalized peptide.

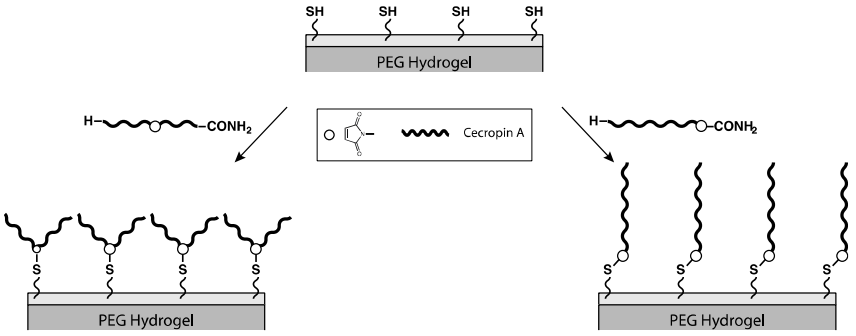

Scheme 2. Immobilization of cecropin A. The antimicrobial peptide cecropin A was affixed to thiol groups on the surfaces of hydrogels via Michael addition with a maleimide functional group positioned either mid-sequence or at the C-terminus of the peptide.

Circular Dichroism Spectroscopy. Circular dichroism (CD) spectroscopic measurements were performed using a Jasco J-1500 CD Spectrometer (190 to 240 nm wavelength scan at 50 nm min^{-1}). For solution-phase measurements, 1 mm pathlength CD cuvettes were filled with 400 μL of aqueous peptide solution (30 μg mL^{-1}) in presence and absence of 50% trifluoroethanol (TFE), which can serve as a biomimetic model for biological membranes, and baseline corrected with a pure solution of water or 50% TFE, respectively. Collected CD ellipticity values (mdeg) were normalized to mean residue ellipticity values ($[\theta]_{MR}$, deg cm^2 $dmol^{-1}$) and fitted with spectra reference SMP180 (optimized for 190–240 nm), a dataset for membrane proteins accessible from the DircroWeb server (http://dichroweb.cryst.bbk.ac.uk/), to analyze secondary structure components.[30] Spectra are reported as the average of 4 scans.

Owing to the inherent absorbance by the hydrogels in the spectral region of interest, CD studies on immobilized peptides were performed using peptides affixed to quartz disks. An acrylic self-assembled monolayer was prepared on the surface of thoroughly cleaned and plasma-treated quartz disks by an overnight incubation in 5% 3-acryloxypropyl trimethoxysilane solution (in ethanol). 4-arm, 10 g mol^{-1} PEGSH was then bound to the surface using a triethylamine-catalyzed Michael Addition, and CPA sequences were conjugated to the free thiols by their maleimide handles in sets of 5. Additionally, 5 slides were left untreated for use as blanks, while 5 more were used to quantify thiol surface density via Ellman's reagent. For immobilized peptide CD analysis, a layer of water or 50% TFE (10 μL) was dispersed between the disks, and CD spectra were collected using the set of 5 untreated disks as a blank. Spectra are presented as the average of 4 scans.

Cell Culture. The bacterial strains employed in this study were *E. coli* K235 (ATCC 13027), *E. coli* serotype O157:H7 (ATCC 700728), and *Shigella sonnei* (ATCC 25931). Cultures were

inoculated on LB agar and incubated overnight at 37°C. An individual colony was isolated from the plate and grown in 15 mL of LB broth at 37°C in a bench top incubator shaker (250 rpm, Innova 4000, New Brunswick Scientific) until late-log phase ($OD_{600} \geq 1.0$). For minimum inhibitory concentration studies, the test inoculum was diluted to 1×10^8 cfu mL^{-1} (~0.06 OD_{670}) in LB broth. Prior to quantifying the antimicrobial activity of the CPA-functionalized hydrogels, cells were washed by centrifugation for 10 min and, after the supernatant was removed, resuspended in sterile 0.85 wt/vol% sodium chloride. This centrifugation/resuspension cycle was repeated twice and, following the final wash, the cells were suspended in a 139 μM glucose solution in modified Davis-Mingioli (DM) growth medium (0.53 wt/vol% potassium phosphate dibasic, 0.2 wt/vol% potassium phosphate monobasic, 0.1 wt/vol% ammonium sulfate, and 0.05 wt/vol% trisodium citrate dihydate). The test inoculum was diluted to a final concentration of 1×10^8 cfu mL^{-1} (~0.06 OD_{670}) for antimicrobial activity quantification.

Minimum Inhibitory Concentration (MIC) Assays. The minimum inhibitory concentrations of CPA solutions were determined in accordance with the protocol outlined by Wiegand *et al.*[31] Briefly, each well of a 96-well polypropylene microtiter plate was inoculated with 90 μL of a 1:200 dilution of the test inoculum. 10 μL of serially-diluted peptide solutions in 0.01% acetic acid and 0.2% BSA over concentrations ranging from 0.1 μg mL^{-1} to 50 μg mL^{-1} were added to the wells of the microtiter plate. The microtiter plates were incubated overnight at 37°C. Cultures without peptide were used as positive controls; uninoculated LB broth was used as a negative control. Minimum inhibitory concentration was defined as the lowest concentration of CPA at which no visible cell growth was observed. Studies were conducted in triplicate.

Antimicrobial activity. The antimicrobial activity of all CPA-functionalized hydrogels against *E. coli* K235 and a single set of CPA-K* functionalized hydrogels (4-arm, 10k g mol^{-1} PEGSH) against *E. coli* O157:H7 and *Shigella* were determined using a microplate reader. Specifically, individual CPA-functionalized hydrogels (and controls) were incubated with 60 μL of test inoculum at 25°C for 3 hr while shaking at 100 rpm. For the bacterial concentration used in this study, 60 μL of test inoculum contains sufficient cells to cover roughly 40% of the surface of a coated hydrogel (d = 3.12 mm, h = 1.56 mm) assuming all cells have an elliptical cross-section (a = 2 μm, b = 1 μm) and are oriented longitudinally along the surface.[32] 10 μL CPA solutions, formulated at concentrations matching the molar quantity of immobilized CPA on their respective hydrogels (i.e., 15 μM, 50 μM, or 135 μM), constituted the positive controls, while coated gels featuring no immobilized CPA served as negative controls. A growth control (60 μL of test inoculum) was also included for comparative purposes. After the 3 hr incubation, 50 μL of the inoculum was withdrawn and combined with 50 μL of LIVE/DEAD *Bac*Light stain (0.3 vol/vol% SYTO 9 and 0.3 vol/vol% propidium iodide in sterile, deionized water) in a fresh 96-well microtiter plate (Costar, black with clear bottom). The microtiter plate was incubated at room temperature in the dark for 15 min. To determine the percent dead cells within each well, the microtiter plate was then exposed to an excitation wavelength of 485 nm, and fluorescence intensities at 530 nm (live cells) and 630 nm (dead cells) were measured such that the ratio of the two intensities could be calculated and compared to signals of a calibration curve generated from known ratios of live:dead bacteria. All studies were performed in triplicate.

Statistical analysis. Results presented herein are expressed as mean ± standard deviation (n = 3). One-way Analysis of Variance (ANOVA) was used to determine statistical significance

between data sets ($\alpha = 0.05$). For data sets with significant differences in means, the Tukey test was applied to identify the source(s) of variation.

RESULTS AND DISCUSSION

Photo-Mediated Polymer Coatings. Cross-linked polymer coatings containing unreacted thiols were formed on the surfaces of PEG hydrogels using an interfacial photo-polymerization technique where the photoinitiator, LAP, and the reactive monomer species, PEGSH and PEGDAE, were initially confined to distinct spatial regions, where LAP was within the hydrogel substrate and the PEG species in the surrounding aqueous immersate solution. Upon UV irradiation, diffusion of radical initiator fragments from the hydrogel core into the aqueous immersate initiated thiol–ene polymerization exclusively at the hydrogel/solution interface, generating conformal polymer coatings. The radical-mediated thiol–ene polymerization mechanism proceeds through alternating propagation and chain transfer events in which thiol and vinyl groups are consumed at equal rates when electron-rich vinyl functional groups, such as vinyl ethers and allyl ethers, are utilized as the ene-bearing monomer (Scheme 3).[33] Consequently, formulating the reactive monomer solutions with a twofold excess of thiols relative to allyl ether functional groups ensured unequal conversion of these functionalities such that abundant unreacted thiols were retained and available for use as peptide immobilization handles in the cross-linked coatings. To visualize the thiolated coating on the cross-linked PEG hydrogel cores, the thiol groups were subjected to Michael addition with a maleimide-functionalized fluorophore and examined using confocal microscopy (see Figure 1).

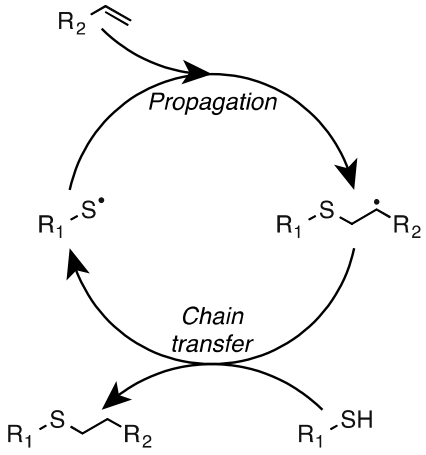

Scheme 3. Thiol–ene reaction mechanism. Upon initiation, the thiol–ene polymerization proceeds via alternating propagation/chain transfer reactions prior to termination. This reaction mechanism assumes ideal conditions in which the alternating steps proceed at the same overall rate.

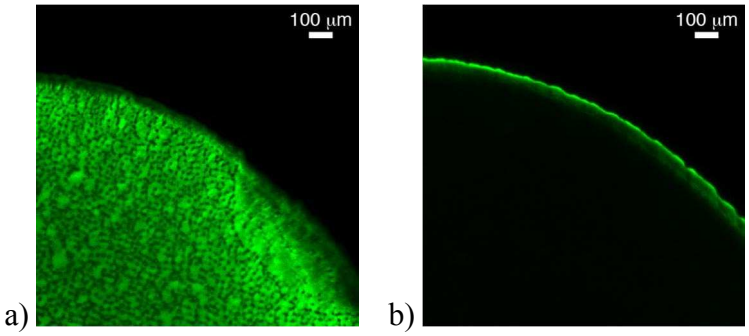

Figure 1. Fluorescent images of coated hydrogels. Here, cross-linked PEG acrylate hydrogel cores were immersed in a 40 wt% monomer solution formulated with 4-arm, 10k g mol^{-1} PEGSH and PEGDAE (SH:C=C, 2:1), irradiated for 35 s, and stained with Alexa Fluor c5 maleimide. Sections were taken at a) the top surface and b) at a depth of 750 μm. Scale bar = 100 μm.

In order to most effectively preserve antimicrobial activity of K*-modified CPA peptides upon immobilization, the surface presentation of the conjugation sites (i.e., thiols) affixed to the coated

hydrogels should enable the bound peptides to approximate the configuration they would adopt in solution. Consequently, the thiol handles used to conjugate the AMPs must be relatively flexible, present in high concentrations, and extend a sufficient distance away from the hydrogel surface for the AMPs to assume an active conformation and penetrate the lipid bilayer of whole cell bacteria as aggregates that induce widespread membrane disruption.[34] The cross-linked polymeric coatings in this study were thus generated from aqueous solutions containing mixtures of flexible, high molecular weight PEGDAE and PEGSH monomers. As illustrated in Scheme 4, the surface presentation of the thiol handles was manipulated by varying the molecular weight and degree of thiol functionalization of the precursor PEGSH, while the surface density of thiol conjugation sites was determined by the overall weight fraction of PEG-based monomer in the immersate solution.

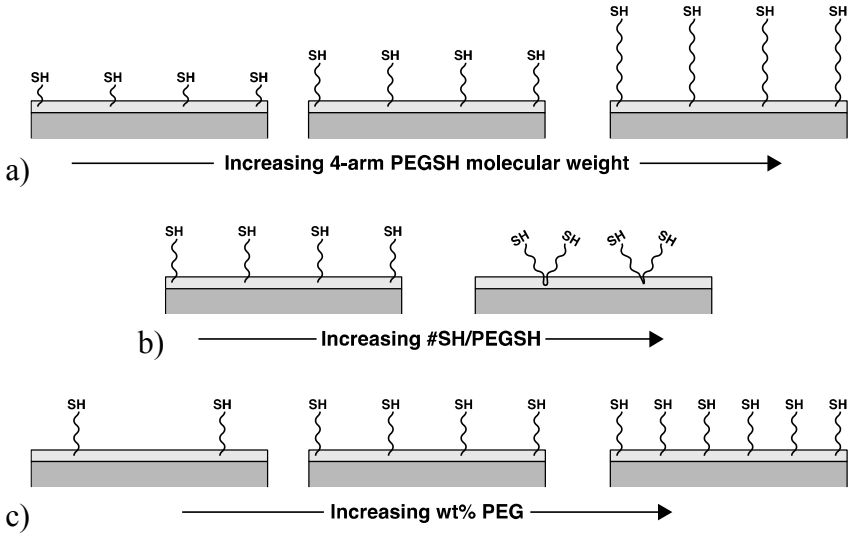

Scheme 4. Surface presentation of thiol handles following interfacial thiol–ene photo-polymerization and illustrated as a function of a) 4-arm PEGSH molecular weight, b) degree of PEGSH thiol functionalization, and c) wt% PEG in 4-arm, 10k g mol^{-1} PEGSH/PEGDAE formulations.

The influence of linker length and functional group clustering on immobilized peptide activity were investigated by preparing coatings generated from PEGSH species of increasing molecular weights (Scheme 4a) and degrees of thiol functionalization (Scheme 4b), respectively. Since each system undergoes interfacial polymerization at a different rate, the duration of light exposure (i.e., the period over which the interfacial polymerization proceeds and coating develops) was tailored for each formulation to afford a final coating thickness of 60 μm. Moreover, the weight fraction of the PEG-based monomers in the aqueous immersate was adjusted such that 0.55 nmol of thiol conjugation sites remained in the cross-linked coating, which corresponded to a final thiol concentration of approximately 410 μM at the target coating volume. The specific weight fractions and exposure times used for each formulation to yield the desired coating thickness and thiol concentration are tabulated in Table 2.

Table 2. PEGSH/PEGDAE pre-polymer formulations, irradiation times, and coating properties.

PEGSH	wt% PEG	Irradiation time (s)	Coating properties	
			Thickness (μm)	Thiol concentration (μM)
4-arm, 5k g mol^{-1}	15	25	61 ± 7	390 ± 60
4-arm, 10k g mol^{-1}	10	60	59 ± 3	90 ± 10
4-arm, 10k g mol^{-1}	20	40	59 ± 4	430 ± 20
4-arm, 10k g mol^{-1}	40	35	61 ± 5	990 ± 230
4-arm, 20k g mol^{-1}	30	48	58 ± 3	410 ± 10
8-arm, 20k g mol^{-1}	20	40	59 ± 6	400 ± 70

Comparison of the requisite UV exposure times among monomer solutions formulated from PEGSH species of differing molecular weights indicates that the rate of coating development

depends on the PEGSH precursor molecular weight. For example, 60 μm thick coatings made from 4-arm PEGSH with molecular weights of 5k, 10k, and 20k g mol^{-1} were generated after 25, 40, and 48 s of UV irradiation, respectively. As the diffusivity of PEG in aqueous solution approximately scales inversely with the square root of its molecular weight,[35] this indicates that the rate at which the interfacial polymerization front advances is limited by diffusion of monomer from the bulk immersate solution to the surface of the gel. Notably, the interaction between reaction and diffusion kinetics in interfacial polymerizations is complex, as is observed for pre-polymer immersate solutions formulated with 8-arm, 20k g mol^{-1} PEGSH. This 8-arm pre-polymer is significantly larger than the 4-arm, 10k g mol^{-1} PEGSH, suggesting that a longer irradiation period would be required for the 20k g mol^{-1} PEGSH to generate an equivalent coating thickness; however, given the significantly lower theoretical gel point conversion for the step growth polymerization of an octafunctional/difunctional comonomer formulation versus a tetrafunctional/difunctional one (53% versus 82%, respectively, for the 2:1 thiol:ene stoichiometric ratio employed here),[36] a nascent, cross-linked coating should be generated earlier in the polymerization for the pre-polymer immersate solution formulated with 8-arm, 20k g mol^{-1} PEGSH. Thus, although a cross-linked gel likely develops more rapidly in close proximity to the core hydrogel surface for 8-arm, 20k g mol^{-1} PEGSH pre-polymer solutions than for those formulated with 4-arm, 10k g mol^{-1} PEGSH, the rate of outward growth is reduced such that both formulations require 40 s of UV irradiation to generate equivalent, 60 μm thick conformal coatings.

To assess the relationship between the surface density of thiol conjugation sites (Scheme 4c) and immobilized peptide activity, the weight fraction of PEG in pre-polymer immersate solutions formulated from PEGDAE and 4-arm, 10k g mol^{-1} PEGSH was varied. For interfacially

photopolymerized coatings using an immersate solution containing 10 wt% PEG, the free thiol concentration was found to be 0.12 ± 0.01 nmol, whereas increasing the monomer content in the immersate to 40 wt% PEG yielded similarly photopolymerized coatings containing 1.3 ± 0.3 nmol free thiol. Since the coating thickness was maintained at 60 μm after polymerization by tailoring the duration of UV irradiation to each formulation, the 10 wt% PEG and 40 wt% PEG formulations afforded thiol concentrations of 90 ± 10 μM and 990 ± 230 μM, respectively, within their polymerized coatings. Kinetic analysis of thiol–ene polymerizations has revealed that such reactions, when performed with allyl ethers as the vinyl group, are chain transfer-limited and proceed as first order reactions with respect to thiol concentration;[37] consequently, the thickness of coatings generated using immersate solutions formulated to contain high thiol concentrations should develop more rapidly than those containing reduced thiol concentrations. Indeed, increasing the monomer content from 10 wt% PEG to 40 wt% PEG did reduce the irradiation period required to generate a 60 μm thick coating by a factor of approximately two, from 60 s to 35 s.

Minimum Inhibitory Concentrations. The antibacterial activity of all CPA sequences that were modified to incorporate a maleimide-bearing lysine residue (i.e., K^*) was evaluated against *E. coli* K235. As the bactericidal activity of CPA has been shown to be sensitive to variations in the chemistry of the N-terminal residues,[38] the first set of modifications to the CPA residue sequence were performed to incorporate the exogenous maleimide-bearing lysine residue, K^*, at the C-terminus. Two additional sequence modifications were constructed based on the active conformation CPA adopts when superficially adsorbed to a bacterial cell membrane.[39] In this state, the peptide folds into a pair of α-helices connected by Ala_{22}–Gly_{23} that serves as a flexible hinge;[40] thus, in a second set of modified CPA sequences, K^* was localized to the hinge region

between Ala_{22} and Gly_{23}. For both sets of sequence modifications, K^* was incorporated in the presence of either preceding or flanking glycine residues to determine if the neutrally charged, flexible spacer prevented unfavorable interactions between K^* and neighboring α-helical or hinge domains. The specific sequences of the four peptides are provided in Table 1.

Prior to surface immobilization, the four modified CPA sequences were screened for activity against *E. coli* K235 by performing broth microdilution assays in the presence of acetic acid/BSA. As shown in Table 1, the lowest MIC (1.56 ± 0.00 μg mL^{-1}) was attained when the maleimide-bearing lysine residue was affixed to the C-terminus of CPA, yielding a peptide with an MIC comparable to that of native CPA against *E. coli* (1.40 μg mL^{-1}).[38] MIC testing was also performed with the CPA-K^* variant against two additional Gram-negative species, *E. coli* O157:H7 and *Shigella sonnei*. MIC values for these microbes were similarly low at 0.23 ± 0.1 μg mL^{-1} and 0.26 ± 0.1 μg mL^{-1}, respectively, indicating the excellent antibacterial activity retention of this peptide against Gram-negative bacterial species. The addition of a 4-glycine bridge at the C-terminus between the native sequence and K^* resulted in little change to the MIC; however, placement of K^* between residues Ala_{22} and Gly_{23} significantly and adversely affected the antibacterial activity of the resultant peptide, yielding an MIC approximately an order of magnitude higher than those of the C-terminus-modified variants. Moreover, inclusion of two glycine residues preceding Ala_{22} and following Gly_{23} further degraded antibacterial activity, resulting in an MIC that exceeded the upper boundary of the test concentrations (>50 μg mL^{-1}).

Solution-phase CD Spectroscopy. Conformational changes in aqueous versus 50% TFE solutions of the 4 modified CPA sequences were investigated using CD spectroscopy, and the results are presented in Figure 2. In aqueous solution, the peptides adopt a mixed secondary structure composed primarily of random coil with β-strands and turns contributing in varying

degrees. The α-helix content within the peptides is minimal in pure water. However, when the peptides are immersed in a biomimetic membrane solution of 50% TFE, the α-helix fraction increases dramatically, indicating that CPA becomes more ordered in the presence of a membrane. The quantity of α-helix correlates with the trend in MIC values in that CPA-K* adopts >90% α-helical structure and displays the lowest MIC while –GGAK*GGG– achieves 20% α-helix and had an MIC value that exceeded the upper boundary of the test range.

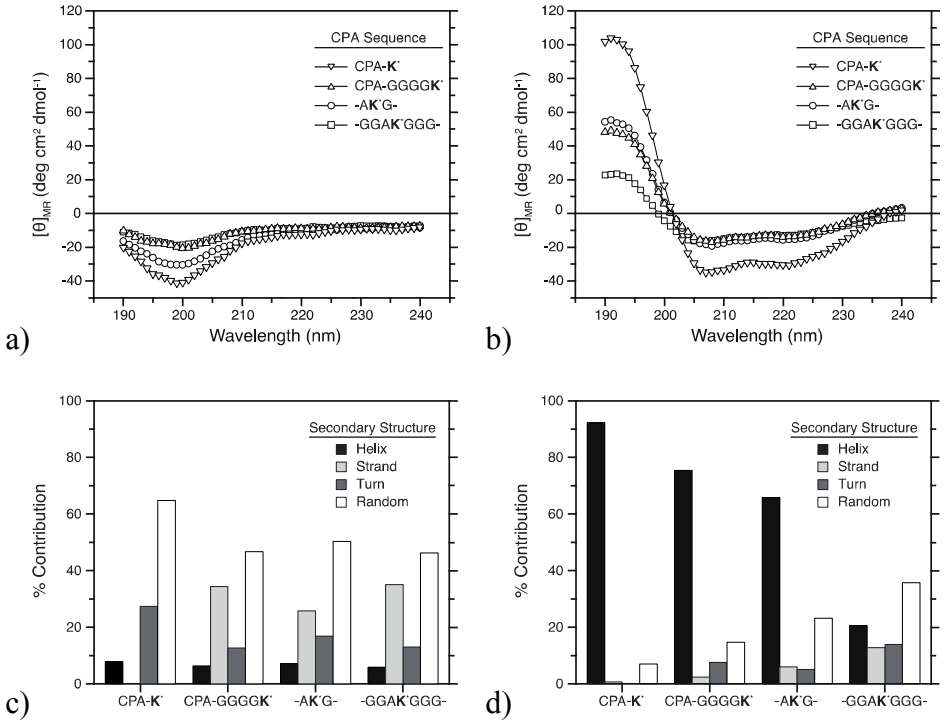

Figure 2. Solution-phase CD spectra for maleimide-modified CPA sequences. Normalized mean residue ellipticity values as a function of wavelength are presented for the peptides in a) aqueous solution and b) in the presence of 50% TFE. Secondary structural contributions for the peptides in c) aqueous solution and d) 50% TFE.

Antimicrobial Activity of Immobilized CPA. Bactericidal activity of hydrogel-immobilized CPA against *E. coli* K235 was quantified, and the results are presented in Figure 3 and Figure 4 as the percentage of dead cells in solution following a 3 hr incubation period. Specifically, the influences of linker length and aggregation on retained antimicrobial activity for the mid-sequence and C-terminus immobilization orientations are depicted in Figure 3a and 3b and Figure 4a and 4b, respectively, whereas the relationship between peptide surface density and activity for hydrogels functionalized with –GGAK*GGG– or CPA–K* is illustrated in Figure 3c and Figure 4c, respectively.

When CPA was immobilized to the coated hydrogel surfaces by a mid-sequence K* (i.e., –AK*G–, Figure 3a), the peptide displayed a dramatic reduction in bactericidal activity relative to the modified peptide in solution regardless of linker length or surface presentation of the PEGSH conjugation handle incorporated in the cross-linked coating. Addition of flanking glycine residues to the "hinge" region (i.e., –GGAK*GGG–, Figure 3b) further decreased the solution-based activity, and the activity of this immobilized CPA sequence was similarly low. However, the mid-sequence immobilized CPA with flanking glycine residues demonstrated a significant reduction in *E. coli* K235 population over coated, unfunctionalized negative control gels at a shorter PEGSH linker length than CPA immobilized at the "hinge" region without glycine spacers. For the –GGAK*GGG– sequence, significant *E. coli* K235 cell death relative to negative controls was observed beginning with the 4-arm, 10k g mol^{-1} PEGSH linker, while significant reduction in *E. coli* K235 population was not seen for the –AK*G– sequence until the 4-arm, 20k g mol^{-1} PEGSH linker was employed..

A significant increase in CPA activity with respect to the PEGSH linker used for peptide immobilization was only observed for coatings generated from 8-arm, 20k g mol^{-1} PEGSH and

featuring the –AGGK*GGG– CPA sequence. Since the high number of thiol functional groups in the 8-arm monomer afforded clusters of flexible conjugation sites within the cross-linked coating, the observed and significant increase in peptide activity from this surface presentation supports the conventional theory that CPA aggregates are necessary to induce widespread membrane disruption and release of intracellular components through the resultant large pores.[41] Regardless, 16 ± 2% dead cells (see Figure 3b, 8-arm, 20k PEGSH) represents a significant loss of peptide activity compared to the 32 ± 3% dead cells observed for the same CPA sequence in solution (Figure 3b, solution). Importantly, as noted in the Materials and Methods, these low death rates cannot be attributed to saturation of the surfaces by the accumulation of dead bacteria as the bacterial loads employed in this study are capable of covering a maximum of 40% of the hydrogel surfaces, which were subjected to agitation over the entire 3 hr incubation period.

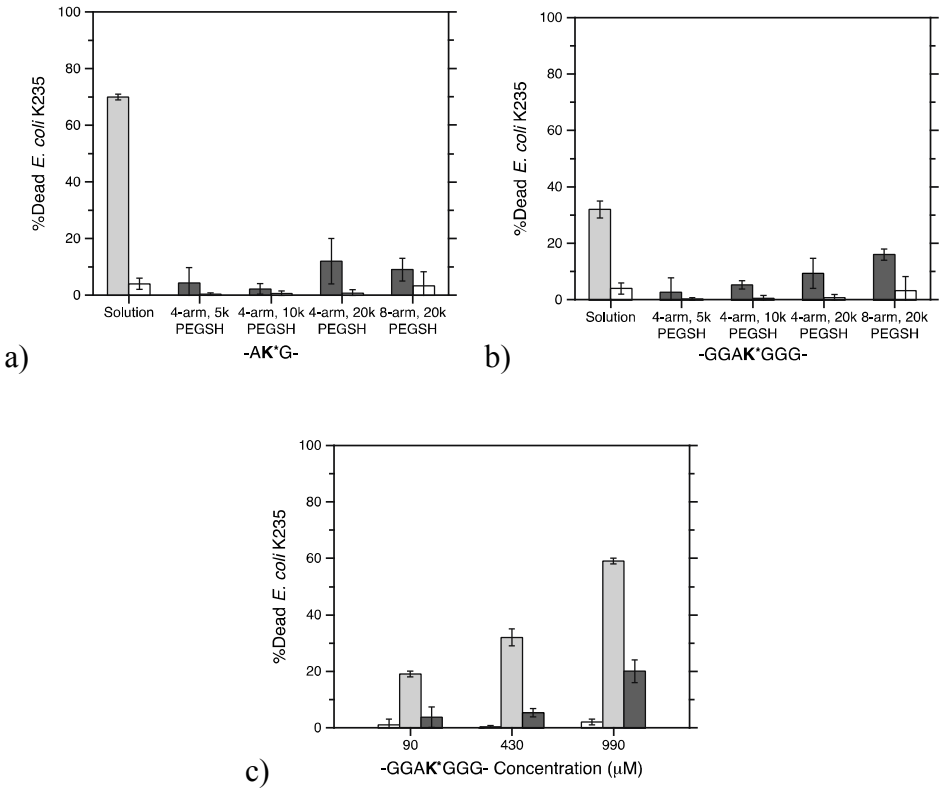

Figure 3. %Dead *E. coli* K235 for CPA sequences modified with a maleimide positioned between the A_{22}–G_{23} residues. Activities of coated, unfunctionalized hydrogels (□), modified CPA sequences free in solution (■), and modified CPA immobilized to coated hydrogels (■) are shown for varying PEGSH linker lengths and functionalization degrees a) without (i.e., –A**K***G–) and b) with flanking Gly spacer residues (–GGA**K***GGG–), or c) to hydrogel coatings generated from 4-arm, 10k g mol^{-1} PEGSH/PEGDAE pre-polymer solutions using 10, 20, or 40 wt% PEG and subsequently surface-functionalized with –GGA**K***GGG– at 90, 430, or 990 μM concentrations, respectively.

The low activity of CPA sequences immobilized to hydrogel substrates by a mid-sequence K* residue is perhaps unsurprising given the high MIC values obtained for these sequences in solution (see Table 1); thus, this low activity may in part be attributed to the location of K* within the native CPA sequence rather than inherent deficiencies associated with the PEGSH linkers. Indeed, localization of the K* residue to the A–G "hinge" region decreased the α-helix content in solution-phase CPA secondary structure immobilized relative to CPA sequences with K* inserted at the C-terminus, although the degree of α-helix content within immobilized –AK*G– appears to be on par with that of CPA immobilized by a C-terminus K* residue (i.e., CPA–K*, Figure 5). At the immobilization test conditions (i.e., 410 μM CPA per gel and 1×10^8 cfu mL^{-1} *E. coli*), the positive control –AK*G– and –GGAK*GGG– CPA solutions were able to kill only 70 ± 1% and 32 ± 3% of the test inoculum, respectively, and once tethered to the hydrogel surfaces exhibited substantial loss of their already low degrees of activity. However, when the surface concentration of –GGAK*GGG– was raised from 90 μM to 990 μM using coatings formulated with 4-arm, 10k g mol^{-1} PEGSH, the bactericidal activity of immobilized –

GGAK*GGG– increased from 3.7 ± 3.6% to 20 ± 4%. The solution-phase –GGAK*GGG– CPA sequence displayed a similar increase in activity, killing 59 ± 4% of the test inoculum at 990 μM versus 32 ± 4% of the test inoculum at 90 μM (Figure 3c); therefore, even at the highest surface density examined, CPA exhibited a loss of nearly two thirds of its solution-phase activity when conjugated by a residue within the hinge region.

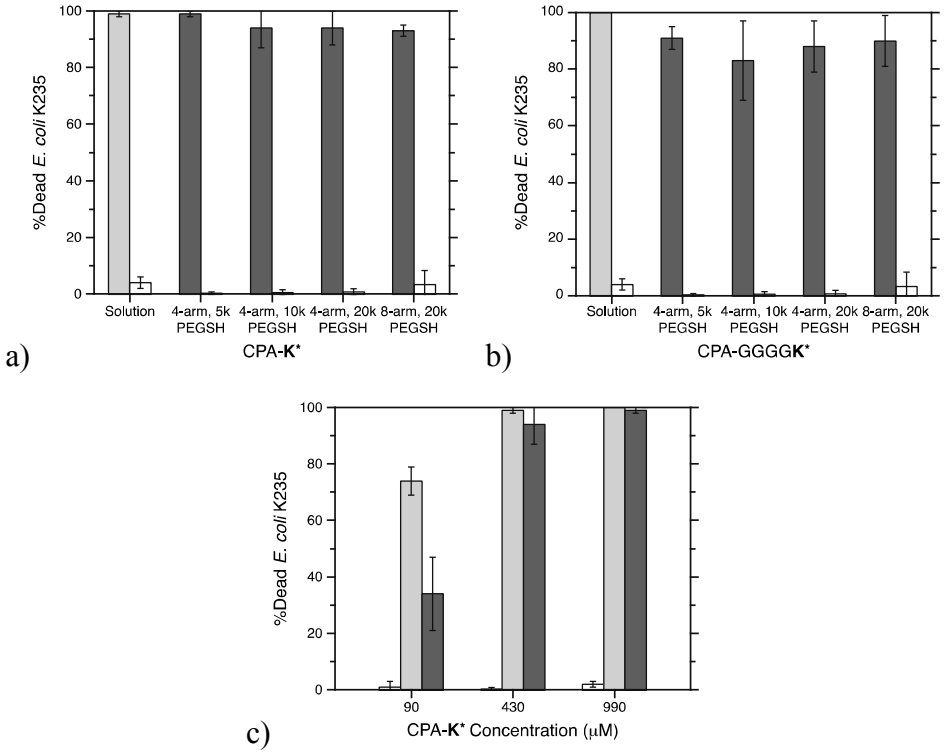

Figure 4. %Dead *E. coli* K235 for CPA sequences modified with a maleimide at the C-terminus. Activities of coated, unfunctionalized hydrogels (□), modified CPA sequences free in solution (■), and modified CPA immobilized to coated hydrogels (■) are shown for varying PEGSH linker lengths and functionalization degrees a) without (i.e., CPA–**K***) and b) with Gly spacer residues (CPA–GGGG**K***), or c) to hydrogel coatings generated from 4-arm, 10k g mol^{-1}

PEGSH/PEGDAE pre-polymer solutions using 10, 20, or 40 wt% PEG and subsequently surface-functionalized with CPA–**K*** at 90, 430, or 990 μM concentrations, respectively.

Although limited antibacterial activity was observed for hydrogels functionalized with CPA via mid-chain K* handles, substantial cell death was seen when the K* residue was affixed to the peptide's C-terminus (Figure 4a and 4b), suggesting that binding CPA from a C-terminal residue affords sufficient rotational freedom for the AMPs to retain antimicrobial activity regardless of the PEGSH linker. CD spectroscopic analysis of the CPA-K* sequence immobilized to the 4-arm, 10k g mol^{-1} PEGSH linker confirmed this assumption; the peaks corresponding to α-helix secondary structure (i.e., negative bands at 208 nm and 222 nm and a positive peak at 193 nm) increase in presence of TFE, indicating that the PEG linker does not prevent the hinged, α-helical conformation from being achieved (see Figure 5). Although the low peptide surface coverage (0.21 ± 0.09 nmol cm^{-2}) precluded sufficient signal strength for quantitative CD spectral analysis, prior work by North and Taitt demonstrated that the α-helical content in CPA bound by a C-terminus cysteine residue is quantitatively equivalent to that of solution-phase CPA.[42]

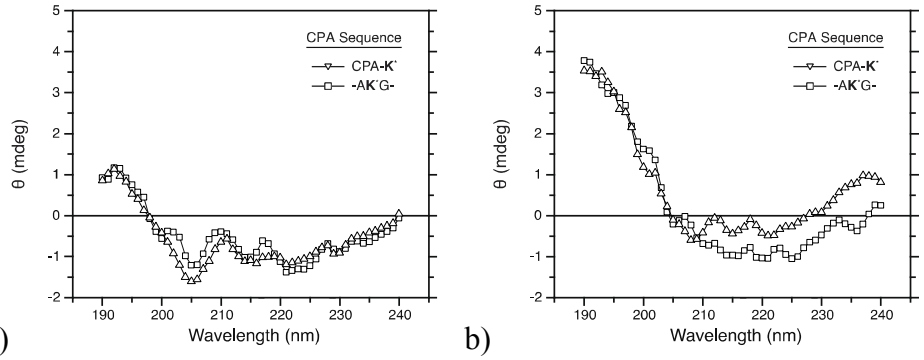

Figure 5. CD spectra for CPA immobilized to quartz via a 4-arm, 10k g mol^{-1} PEGSH. CD ellipticity values as a function of wavelength are presented for the immobilized peptides immersed in a) aqueous solution and b) in the presence of 50% TFE.

As seen in Figure 4c and 4d, the greatest dead cell percentages for the linkers examined were observed when CPA–K* (99 ± 1%) and CPA–GGGGK* (91 ± 4%) were bound to coatings formulated with 4-arm, 5k g mol^{-1} PEGSH. Increasing the linker length caused a slight decrease in *E. coli* K235 cell death for both bound CPA sequences, but these changes were not statistically significant. Moreover, using 8-arm, 20k g mol^{-1} PEGSH in place of 4-arm, 10k g mol^{-1} PEGSH to spatially aggregate immobilized peptides had negligible impact on the anti-*E. coli* activity of CPA–K* and a statistically insignificant improvement in the activity of CPA–GGGGK*. Finally, no significant difference was observed between CPA–K* and CPA–GGGGK* activity when the peptides were immobilized to identical hydrogel surfaces, irrespective of the employed linker, indicating that the Gly spacer does not provide any additional, advantageous conformational freedom. Although the hydrogel surface area to bacterial load ratio employed in this work prevented surface saturation by the pathogen, a distinct advantage of PEG-based hydrogels as AMP immobilization platforms is their inherent resistance to fouling,[43] enabling their use under bacterial loads that would otherwise saturate the polymer surface with debris from dead bacteria and facilitate reusability.

The insignificant variation in the activity of C-terminus-immobilized CPA for the PEGSH linkers examined may be attributed to the linker lengths all being at or above the critical threshold for the peptide to effectively form cytotoxic pores in *E. coli* cell membranes. Recent work demonstrated that the mechanism of action for immobilized chrysophsin-1, a histidine-rich

AMP, is mediated by the molecular weight of the PEG-based surface linker.[44] When immobilized by a PEG linker with a molecular weight of less than 1k g mol^{-1}, chrysophsin-1 destabilized bacterial membranes by cation displacement; however, for a 7.5k g mol^{-1} PEG linker, the AMP was able to generate pores in the bacterial membrane and thus display increased antibacterial activity. Given that CPA activity against *E. coli* K235 was highest using 4-arm, 5k g mol^{-1} PEGSH, one may infer that the AMP's mechanism of action is predominantly membrane pore formation at linear PEGSH molecular weights of 2.5k g mol^{-1} and above.

To further illustrate the relationship between the peptide surface and its degree of retained activity, the surface density of C-terminus immobilized CPA (CPA–K^*, Figure 4c) using 4-arm, 10k g mol^{-1} PEGSH as the linker was varied and the antimicrobial activity of the resultant surfaces was measured. When the surface concentration of CPA–K^* was set at 90 ± 10 μM, the immobilized peptide demonstrated a 54% loss of antimicrobial activity relative to its activity when free in solution; however, as the surface concentration was increased to 430 ± 20 μM and 990 ± 230 μM, the immobilized CPA retained 96% and 98% of its antibacterial activity, respectively. This suggests that a threshold surface concentration exists at which CPA maintains a high degree of its solution-based activity upon immobilization and, for CPA–K^*, this value is between 90 and 430 μM, but for –GGAK^*GGG–, the concentration is above 990 μM. The degree of immobilized CPA activity against two additional Gram-negative pathogens, *E. coli* O157:H7 and *Shigella sonnei*, was measured to demonstrate the retained activity breadth when bound to a surface. CPA-K^* immobilized at 430 ± 20 μM using 4-arm, 10k g mol^{-1} PEGSH as the linker killed 99.9 ± 0.1% of the *E. coli* O157:H7 population, nearly a 3-log reduction, and >99.9% of the *Shigella* population following a 3 hr incubation. These values approached the activities observed in positive control solutions which eliminated 100% of both bacteria under

identical test conditions, whereas the bacteria populations increased in the presence of coated, unfunctionalized negative control gels. This high degree of antibacterial activity retained by CPA upon C-terminus hydrogel immobilization indicates that the platform could be employed as a broad-spectrum decontaminant against Gram-negative species.

5. Conclusions

Interfacial photo-polymerization provides a facile route to immobilize AMPs in active conformations to the surface of pre-fabricated hydrogels. Selection of monomers in the pre-polymer solution enables surface concentration and presentation to be tailored to a given peptide such that antimicrobial activity can be optimized for specific pathogens. Here, PEG monomers were used in the monomer solution to ensure linker flexibility such that immobilized CPA molecules could adopt the active, hinged α-helical conformation when bound by a C-terminal or mid-hinge K^* residue, as confirmed by CD spectroscopy. Solution MIC proved valuable for predicting the antimicrobial behavior of CPA immobilized at varying locations in the peptide sequence and against an assortment of Gram-negative bacterial species. When K^* was inserted between the A_{22}–G_{23} residues, the MIC was 25 μg mL^{-1}; however, when K^* was positioned at the C-terminus, over a tenfold lower MIC of 1.56 μg mL^{-1} was observed. Although addition of Gly spacers negatively impacted the MIC of CPA against *E. coli* K235 in both orientations, the effect was more pronounced for the mid-sequence modified peptide, which had an MIC outside of the maximum concentration limit. The MICs of *E. coli* O157: H7 and *Shigella sonnei* for the CPA sequence with K^* positioned at the C-terminus without Gly spacers were the lowest observed in this study. These trends in MIC were reflected in the antimicrobial activity of CPA upon surface immobilization, where modified CPA sequences with the higher MIC values displayed lower degrees of bacterial cell death both in solution and bound to hydrogel surfaces than modified

sequences with low MIC values. The relationship between linker type and bactericidal activity towards *E. coli* K235 was found to be more influential for the mid-sequence modified CPA, where the degree of *E. coli* cell death was directly related to linker length and degree of thiol functionalization. Nevertheless, bactericidal results from both immobilization locales indicate that Gly spacers do not substantially improve CPA activity when affixed by high M_n PEG linkers and that surface concentration is the critical parameter for retaining antibacterial activity.

AUTHOR INFORMATION

Corresponding Author

* Tel.: +1 734 763 3493, fax: +1 734 763 0459, e-mail: tfscott@umich.edu.

* Tel.: +1 508 233 5825, fax: +1 508 233 5527, e-mail: charlene.m.mello2.civ@mail.mil.

Author Contributions

The manuscript was written through contributions of all authors. All authors have given approval to the final version of the manuscript.

Notes

The authors declare no competing financial interest.

ACKNOWLEDGMENT

This work has been support by funding from the Defense Threat Reduction Agency and was performed while MAC held an NRC Research Associateship award at the US Army Natick

Soldier Research, Development and Engineering Center (NSRDEC). This manuscript has been approved for unlimited distribution by the US Army NSRDEC (PAO #: U15-340). The authors would also like to thank the Department of Chemistry and Biochemistry at the University of Massachusetts, Dartmouth for the use of their facilities, Prof. Zhan Chen at the Department of Chemistry, University of Michigan, for the use of his CD spectrometer, and J. Jasensky for his assistance with the CD experiments.

ABBREVIATIONS

AMP antimicrobial peptide; CPA cecropin A; PEG poly(ethylene glycol); PEGDA poly(ethylene glycol) diacrylate; PEGDAE poly(ethylene glycol) diallyl ether; PEGSH thiolated poly(ethylene glycol).

REFERENCES

(1) Kuttner, A. G., Production of Bacteriocines by Group a Streptococci with Special Reference to Nephritogenic Types. *J. Exp. Med.* **1966**, *124*, 279-291, DOI:10.1084/jem.124.3.279.

(2) Fernandez de Caleya, R.; Gonzalez-Pascual, B.; Garcia-Olmedo, F.; Carbonero, P., Susceptibility of Phytopathogenic Bacteria to Wheat Purothionins in Vitro. *Appl. Microbiol.* **1972**, *23*, 998-1000.

(3) Hultmark, D.; Steiner, H.; Rasmuson, T.; Boman, H. G., Insect Immunity - Purification and Properties of 3 Inducible Bactericidal Proteins from Hemolymph of Immunized Pupae

of Hyalophora-Cecropia. *Eur. J. Biochem.* **1980**, *106*, 7-16, DOI:10.1111/j.1432-1033.1980.tb05991.x.

(4) Schittek, B.; Hipfel, R.; Sauer, B.; Bauer, J.; Kalbacher, H.; Stevanovic, S.; Schirle, M.; Schroeder, K.; Blin, N.; Meier, F.; Rassner, G.; Garbe, C., Dermcidin: A Novel Human Antibiotic Peptide Secreted by Sweat Glands. *Nat. Immunol.* **2001**, *2*, 1133-1137, DOI:10.1038/ni732.

(5) Hoskin, D. W.; Ramamoorthy, A., Studies on Anticancer Activities of Antimicrobial Peptides. *Biochim. Biophys. Acta* **2008**, *1778*, 357-375, DOI:10.1016/j.bbamen.2007.11.008.

(6) Friedrich, C. L.; Rozek, A.; Patrzykat, A.; Hancock, R. E., Structure and Mechanism of Action of an Indolicidin Peptide Derivative with Improved Activity against Gram-Positive Bacteria. *J. Biol. Chem.* **2001**, *276*, 24015-24022, DOI:10.1074/jbc.M009691200.

(7) Hancock, R. E.; Chapple, D. S., Peptide Antibiotics. *Antimicrob. Agents Chemother.* **1999**, *43*, 1317-1323, DOI:10.1016/S0140-6736(97)80051-7.

(8) Shai, Y., Mechanism of the Binding, Insertion and Destabilization of Phospholipid Bilayer Membranes by Alpha-Helical Antimicrobial and Cell Non-Selective Membrane-Lytic Peptides. *Biochim. Biophys. Acta, Biomembr.* **1999**, *1462*, 55-70, DOI:10.1016/s0005-2736(99)00200-x.

(9) Goumon, Y.; Lugardon, K.; Kieffer, B.; Lefevre, J.; Van Dorsselaer, A.; Aunis, D.; Metz-Boutigue, M., Characterization of Antibacterial Cooh-Terminal Proenkephalin-A-Derived

Peptides (PEAP) in Infectious Fluids. *J. Biol. Chem.* **1998**, *273*, 29847-29856, DOI:10.1074/jbc.273.45.29847.

(10) (a) Scocchi, M.; Tossi, A.; Gennaro, R., Proline-Rich Antimicrobial Peptides: Converging to a Non-Lytic Mechanism of Action. *Cell. Mol. Life Sci.* **2011**, *68*, 2317-2330, DOI:10.1007/s00018-011-0721-7; (b) Ilic, N.; Novkovic, M.; Guida, F.; Xhindoli, D.; Benincasa, M.; Tossi, A.; Juretic, D., Selective Antimicrobial Activity and Mode of Action of Adepantins, Glycine-Rich Peptide Antibiotics Based on Anuran Antimicrobial Peptide Sequences. *Biochim. Biophys. Acta, Biomembr.* **2013**, *1828*, 1004-1012, DOI:10.1016/j.bbamem.2012.11.017.

(11) Mor, A.; Hani, K.; Nicolas, P., The Vertebrate Peptide Antibiotics Dermaseptins Have Overlapping Structural Features but Target Specific Microorganisms. *J. Biol. Chem.* **1994**, *269*, 31635-31641.

(12) Ganz, T.; Selsted, M.; Szklarek, D.; Harwig, S.; Daher, K., Defensins - Natural Peptide Antibiotics of Human-Neutrophils. *J. Clin. Invest.* **1985**, *76*, 1427-1435, DOI:10.1172/JCI112120.

(13) Chernysh, S.; Kim, S. I.; Bekker, G.; Pleskach, V. A.; Filatova, N. A.; Anikin, V. B.; Platonov, V. G.; Bulet, P., Antiviral and Antitumor Peptides from Insects. *Proc. Natl. Acad. Sci. U. S. A.* **2002**, *99*, 12628-12632, DOI:10.1073/pnas.192301899.

(14) (a) Cruciani, R. A.; Barker, J. L.; Zasloff, M.; Chen, H. C.; Colamonici, O., Antibiotic Magainins Exert Cytolytic Activity against Transformed Cell Lines through Channel Formation. *Proc. Natl. Acad. Sci. U. S. A.* **1991**, *88*, 3792-3796, DOI:10.1073/pnas.88.9.3792; (b) Utsugi, T.; Schroit, A. J.; Connor, J.; Bucana, C. D.;

Fidler, I. J., Elevated Expression of Phosphatidylserine in the Outer Membrane Leaflet of Human Tumor Cells and Recognition by Activated Human Blood Monocytes. *Cancer Res.* **1991**, *51*, 3062-3066, ; (c) Yoon, W.; Park, H.; Lim, K.; Hwang, B., Effect of O-Glycosylated Mucin on Invasion and Metastasis of Hm7 Human Colon Cancer Cells. *Biochem. Biophys. Res. Commun.* **1996**, *222*, 694-699, DOI:10.1006/bbrc.1996.0806; (d) Hoskin, D. W.; Ramamoorthy, A., Studies on Anticancer Activities of Antimicrobial Peptides. *Biochim. Biophys. Acta, Biomembr.* **2008**, *1778*, 357-375, DOI:10.1016/j.bbamem.2007.11.008.

(15) Kulagina, N. V.; Lassman, M. E.; Ligler, F. S.; Taitt, C. R., Antimicrobial Peptides for Detection of Bacteria in Biosensor Assays. *Anal. Chem.* **2005**, *77*, 6504-6508, DOI:10.1021/ac050639r.

(16) Etayash, H.; Norman, L.; Thundat, T.; Kaur, K., Peptide-Bacteria Interactions Using Engineered Surface-Immobilized Peptides from Class IIa Bacteriocins. *Langmuir* **2013**, *29*, 4048-4056, DOI:10.1021/la3041743.

(17) Appendini, P.; Hotchkiss, J. H., Surface Modification of Poly(Styrene) by the Attachment of an Antimicrobial Peptide. *J. Appl. Polym. Sci.* **2001**, *81*, 609-616, DOI:10.1002/app.1476.

(18) Sitaram, N.; Nagaraj, R., Interaction of Antimicrobial Peptides with Biological and Model Membranes: Structural and Charge Requirements for Activity. *Biochim. Biophys. Acta, Biomembr.* **1999**, *1462*, 29-54, DOI:10.1016/S0005-2736(99)00199-6.

(19) Kulagina, N. V.; Shaffer, K. M.; Anderson, G. P.; Ligler, F. S.; Taitt, C. R., Antimicrobial Peptide-Based Array for *Escherichia Coli* and *Salmonella* Screening. *Anal. Chim. Acta* **2006**, *575*, 9-15, DOI:10.1016/j.aca.2006.05.082.

(20) (a) Glinel, K.; Jonas, A. M.; Jouenne, T.; Leprince, J.; Galas, L.; Huck, W. T. S., Antibacterial and Antifouling Polymer Brushes Incorporating Antimicrobial Peptide. *Bioconjugate Chem.* **2008**, *20*, 71-77, DOI:10.1021/bc800280u; (b) Uzarski, J. R.; Mello, C. M., Detection and Classification of Related Lipopolysaccharides Via a Small Array of Immobilized Antimicrobial Peptides. *Anal. Chem.* **2012**, *84*, 7359-7366, DOI:10.1021/ac300987h; (c) Lim, K.; Chua, R. R. Y.; Saravanan, R.; Basu, A.; Mishra, B.; Tambyah, P. A.; Ho, B.; Leong, S. S., Immobilization Studies of an Engineered Arginine-Tryptophan-Rich Peptide on a Silicon Surface with Antimicrobial and Antibiofilm Activity. *ACS Appl. Mater. Interfaces* **2013**, *5*, 6412-6422, DOI:10.1021/am401629p.

(21) (a) Uzarski, J. R.; Tannous, A.; Morris, J. R.; Mello, C. M., The Effects of Solution Structure on the Surface Conformation and Orientation of a Cysteine-Terminated Antimicrobial Peptide Cecropin P1. *Colloids Surf., B* **2008**, *67*, 157-165, DOI:10.1016/j.colsurfb.2008.07.011; (b) Strauss, J.; Kadilak, A.; Cronin, C.; Mello, C. M.; Camesano, T. A., Binding, Inactivation, and Adhesion Forces between Antimicrobial Peptide Cecropin P1 and Patogenic *E. Coli*. *Colloids Surf., B* **2010**, *75*, 156-164, DOI:10.1016/j.colsurfb.2009.08.026; (c) Mannoor, M. S.; Zhang, S. Y.; Link, A. J.; McAlpine, M. C., Electrical Detection of Pathogenic Bacteria Via Immobilized Antimicrobial Peptides. *Proc. Natl. Acad. Sci. U. S. A.* **2010**, *107*, 19207-19212, DOI:10.1073/pnas.1008768107.

(22) (a) Han, X. F.; Soblosky, L.; Slutsky, M.; Mello, C. M.; Chen, Z., Solvent Effect and Time-Dependent Behavior of C-Terminus-Cysteine-Modified Cecropin P1 Chemically Immobilized on a Polymer Surface. *Langmuir* **2011**, *27*, 7042-7051, DOI:10.1021/la200388y; (b) Han, X. F.; Uzarski, J. R.; Mello, C. M.; Chen, Z., Different Interfacial Behaviors of N- and C-Terminus Cysteine-Modified Cecropin P1 Chemically Immobilized onto Polymer Surface. *Langmuir* **2013**, *29*, 11705-11712, DOI:10.1021/la401818k.

(23) (a) Gabriel, M.; Nazmi, K.; Veerman, E. C.; Amerongen, A. V. N.; Zentner, A., Preparation of Ll-37-Grafted Titanium Surfaces with Bactericidal Activity. *Bioconjugate Chem.* **2006**, *17*, 548-550, DOI:10.1021/bc050091v; (b) Cho, W. M.; Joshi, B. P.; Cho, H.; Lee, K. H., Design and Synthesis of Novel Antibacterial Peptide-Resin Conjugates. *Bioorg. Med. Chem. Lett.* **2007**, *17*, 5772-5776, DOI:10.1016/j.bmcl.2007.08.056.

(24) Santos, C. M.; Kumar, A.; Kolar, S. S.; Contreras-Caceres, R.; McDermott, A.; Cai, C., Immobilization of Antimicrobial Peptide Ig-25 onto Fluoropolymers Via Fluorous Interactions and Click Chemistry. *ACS Appl. Mater. Interfaces* **2013**, *5*, 12789-12793, DOI:10.1021/am404591n.

(25) Steven, M. D.; Hotchkiss, J. H., Covalent Immobilization of an Antimicrobial Peptide on Poly(Ethylene) Film. *J. Appl. Polym. Sci.* **2008**, *110*, 2665-2670, DOI:10.1002/app.27638.

(26) Ivanov, I. E.; Morrison, A. E.; Cobb, J. E.; Fahey, C. A.; Camesano, T. A., Creating Antibacterial Surfaces with the Peptide Chrysophsin-1. *ACS Appl. Mater. Interfaces* **2012**, *4*, 5891-5897, DOI:10.1021/am301530a.

(27) Majima, T.; Schnabel, W., Phenyl-2,4,6-Trimethylbenzoylphosphinates as Water-Soluble Photoinitiators. Generation and Reactivity of $O=P(C_6h_5)(O^-)$ Radical Anions. *Makromol. Chem.* **1991**, *192*, 2307-2315, DOI:10.1002/macp.1991.021921010.

(28) Scott, T. F.; Kloxin, C. J.; Draughon, R. B.; Bowman, C. N., Nonclassical Dependence of Polymerization Rate on Initiation Rate Observed in Thiol−Ene Photopolymerizations. *Macromolecules* **2008**, *41*, 2987-2989, DOI:10.1021/ma8002505.

(29) Riddles, P. W.; Blakeley, R. L.; Zerner, B., Reassessment of Ellman's Reagent. *Meth. Enzymol.* **1983**, *91*, 49-60, DOI:10.1016/S0076-6879(83)91010-8.

(30) Abdul-Gader, A.; Miles, A. J.; Wallace, B. A., A Reference Dataset for the Analyses of Membrane Protein Secondary Structures and Transmembrane Residues Using Circular Dichroism. *Bioinformatics* **2011**, *27*, 1630-1636, DOI:10.1093/bioinformatics/btr234.

(31) Wiegand, I.; Hilpert, K.; Hancock, R. E. W., Agar and Broth Dilution Methods to Determine the Minimal Inhibitory Concentration (Mic) of Antimicrobial Substances. *Nat. Protocols* **2008**, *3*, 163-175, DOI:10.1038/nprot.2007.521.

(32) Phillips, R.; Kondev, J.; Theriot, J.; Garcia, H. G. In *Physical Biology of the Cell*, 2nd ed.; Scholl, S., Ed.; Garland Science: London and New York, 2012; p 26.

(33) Hoyle, C. E.; Bowman, C. N., Thiol-Ene Click Chemistry. *Angew. Chem., Int. Ed.* **2010**, *49*, 1540-1573, DOI:10.1002/anie.200903924.

(34) Silvestro, L.; Weiser, J. N.; Axelsen, P. H., Antibacterial and Antimembrane Activities of Cecropin A in Escherichia Coli. *Antimicrob. Agents Chemother.* **2000**, *44*, 602-607, DOI:10.1128/aac.44.3.602-607.2000.

(35) Shimada, K.; Kato, H.; Saito, T.; Matsuyama, S.; Kinugasa, S., Precise Measurement of the Self-Diffusion Coefficient for Poly(Ethylene Glycol) in Aqueous Solution Using Uniform Oligomers. *J. Chem. Phys.* **2005**, *122*, 7, DOI:10.1063/1.1948378.

(36) (a) Flory, P. J., Molecular Size Distribution in Three Dimensional Polymers. I. Gelation. *J. Am. Chem. Soc.* **1941**, *63*, 3083-3090, DOI:10.1021/ja01856a061; (b) Stockmayer, W. H., Theory of Molecular Size Distribution and Gel Formation in Branched-Chain Polymers. *J. Chem. Phys.* **1943**, *11*, 45-55, DOI:10.1063/1.1723803.

(37) Cramer, N. B.; Reddy, S. K.; O'Brien, A. K.; Bowman, C. N., Thiol−Ene Photopolymerization Mechanism and Rate Limiting Step Changes for Various Vinyl Functional Group Chemistries. *Macromolecules* **2003**, *36*, 7964-7969, DOI:10.1021/ma034667s.

(38) Andreu, D.; Merrifield, R. B.; Steiner, H.; Boman, H. G., N-Terminal Analogs of Cecropin A: Synthesis, Antibacterial Activity, and Conformational Properties. *Biochemistry* **1985**, *24*, 1683-1688, DOI:10.1021/bi00328a017.

(39) Silvestro, L.; Axelsen, P. H., Membrane-Induced Folding of Cecropin A. *Biophys. J.* **2000**, *79*, 1465-1477, DOI:10.1016/S0006-3495(00)76398-3.

(40) Holak, T. A.; Engstrom, A.; Kraulis, P. J.; Lindeberg, G.; Bennich, H.; Jones, T. A.; Gronenborn, A. M.; Clore, G. M., The Solution Conformation of the Antibacterial Peptide Cecropin A: A Nuclear Magnetic Resonance and Dynamical Simulated Annealing Study. *Biochemistry* **1988**, *27*, 7620-7629, DOI:10.1021/bi00420a008.

(41) Silvestro, L.; Gupta, K.; Weiser, J. N.; Axelsen, P. H., The Concentration-Dependent Membrane Activity of Cecropin A. *Biochemistry* **1997**, *36*, 11452-11460, DOI:10.1021/bi9630826.

(42) North, S. H.; Taitt, C. R., Application of Circular Dichroism for Structural Analysis of Surface-Immobilized Cecropin a Interacting with Lipoteichoic Acid. *Langmuir* **2015**, *31*, 10791-10798, DOI:10.1021/acs.langmuir.5b02600.

(43) (a) Li, P.; Poon, Y. F.; Weifeng, L.; Zhu, H. Y.; Yeap, S. H.; Cao, Y.; Qi, X.; Zhou, C.; Lamrani, M.; Beuerman, R. W.; Kang, E. T.; Mu, Y.; Li, C. M.; Chang, M. W.; Leong, S. S.; Chan-Park, M. B., A Polycationic Antimicrobial and Biocompatible Hydrogel with Microbe Membrane Suctioning Ability. *Nat. Mater.* **2011**, *10*, 149-156, DOI:10.1038/NMAT2915. (b) Liu, S. Q.; Yang, C.; Huang, Y.; Ding, X.; Yan, L.; Wei, M. F.; Hedrick, J. L.; Yang, Y., Antimicrobial and Antifouling Hydrogels Formed in Situ from Polycarbonate and Poly(Ethylene Glycol) Via Michael Addition. *Adv. Mater.* **2012**, *24*, 6484-6489, DOI:10.1002/adma.201202225.

(44) Lozeau, L. D.; Alexander, T. E.; Camesano, T. A., Proposed Mechanisms of Tethered Antimicrobial Peptide Chrysophsin-1 as a Function of Tether Length Using Qcm-D. *J. Phys. Chem. B* **2015**, *119*, 13142-13151, DOI:10.1021/acs.jpcb.5b06883.

For Table of Contents Use Only

Bactericidal Hydrogels via Surface Functionalization with Cecropin A

Cole, Megan; Scott, Timothy; Mello, Charlene